NASA TECHNICAL NOTE

NASA TN D-6083

A METHOD FOR ANALYZING THE INTERACTION OF AN OBLIQUE SHOCK WAVE WITH A BOUNDARY LAYER

by William C. Rose

Ames Research Center
Moffett Field, Calif. 94035

NATIONAL AERONAUTICS AND SPACE ADMINISTRATION • WASHINGTON, D. C. • NOVEMBER 1970

1. Report No. NASA TN D-6083	2. Government Accession No.	3. Recipient's Catalog No.
4. Title and Subtitle A METHOD FOR ANALYZING THE INTERACTION OF AN OBLIQUE SHOCK WAVE WITH A BOUNDARY LAYER		5. Report Date November 1970 6. Performing Organization Code
7. Author(s) William C. Rose		8. Performing Organization Report No. A-3714 10. Work Unit No. 722-03-10-08-00-21
9. Performing Organization Name and Address NASA Ames Research Center Moffett Field, Calif. 94035		11. Contract or Grant No.
12. Sponsoring Agency Name and Address National Aeronautics and Space Administration Washington, D. C. 20546		13. Type of Report and Period Covered Technical Note 14. Sponsoring Agency Code

15. Supplementary Notes

16. Abstract

A method is presented for predicting the characteristics of an interaction produced by an externally generated, oblique shock wave that impinges on either laminar or turbulent boundary layers. The basis of the method is the assumption that the boundary layer in the interaction region may be divided into two layers: the outer layer, an essentially inviscid but rotational layer, and the inner layer, an essentially viscous layer. Coupling of the inner and outer flows throughout the interaction region is discussed. The only empirical information required for using the method is the extent of upstream propagation of the pressure rise. Correlations for the length of upstream influence, based on parameters consistent with the two-layer hypothesis, are presented in the appendix. Results predicted by the method are compared with experimental results in terms of surface pressure distributions, heat transfer, and flow-field configuration (*i.e.*, shock-wave structure and regions of compression and expansion).

17. Key Words (Suggested by Author(s)) Turbulent boundary layer Laminar boundary layer Shock-wave interaction	18. Distribution Statement Unclassified–Unlimited

19. Security Classif. (of this report) Unclassified	20. Security Classif. (of this page) Unclassified	21. No. of Pages 16	22. Price* $3.00

*For sale by the Clearinghouse for Federal Scientific and Technical Information
Springfield, Virginia 22151

SYMBOLS

C_f	local skin-friction coefficient
M	Mach number
M_o	Mach number at boundary-layer edge at onset of pressure rise
p	local pressure
q	heat-transfer rate from surface per unit area
Re	Reynolds number
T	temperature
x	distance along surface from leading edge
y	distance normal to surface
$y_{viscous}$	sublayer thickness
α_L	local flow turning angle across incident shock wave
δ	boundary-layer thickness
δ_M	boundary-layer thickness determined by Mach number profile (fig. 1)
δ_{T_t}	boundary-layer thickness determined by total-temperature profile (fig. 1)

Subscripts

final	downstream of interaction
i	station where incident shock intersects viscous layer (see figs. 12 and 13)
o	conditions at onset of pressure rise
p	plateau
t	total conditions
δ	boundary-layer edge

A METHOD FOR ANALYZING THE INTERACTION OF AN OBLIQUE SHOCK WAVE WITH A BOUNDARY LAYER

William C. Rose

Ames Research Center

SUMMARY

A method is presented for predicting the characteristics of an interaction produced by an externally generated, oblique shock wave that impinges on either laminar or turbulent boundary layers. The basis of the method is the assumption that the boundary layer in the interaction region may be divided into two layers: the outer layer, an essentially inviscid but rotational layer, and the inner layer, an essentially viscous layer. Coupling of the inner and outer flows throughout the interaction region is discussed. The only empirical information required for using the method is the extent of upstream propagation of the pressure rise. Correlations for the length of upstream influence, based on parameters consistent with the two-layer hypothesis, are presented in the appendix. Results predicted by the method are compared with experimental results in terms of surface pressure distributions, heat transfer, and flow-field configuration (*i.e.*, shock-wave structure and regions of compression and expansion).

INTRODUCTION

For aircraft that are to fly at supersonic and hypersonic Mach numbers, interactions between oblique shock waves and boundary layers must be properly accounted for to predict adequately the external aerodynamics as well as the internal aerodynamics of engine inlets. Assessing aerodynamic performance requires knowledge of the details of the interaction of a shock wave with a boundary layer, such as the manner in which the boundary layer develops throughout an interaction, and how the flow external to the boundary layer is modified as a result of the interaction. It is important to know whether or not the boundary layer will separate when subjected to the shock-induced pressure rise. Typical modifications of the external flow field would be regions of compression and expansion induced by the interaction. These modifications are of paramount importance in internal flows, since the characteristics of the reflected compression and expansion regions originating at an interaction on one wall of an engine inlet must be known to determine the character of the flow field that interacts with the boundary layer on the opposite wall. Various proposed methods of analyzing these interactions are briefly reviewed below.

A method for analyzing the flow resulting from an oblique shock wave impinging on a turbulent boundary layer was presented in reference 1. This method was based on the assumption that the effects of viscosity on the interaction region could be neglected. Thus, the mathematical modeling was taken in the spirit of Lighthill's 1950 paper (ref. 2). In this work he treated the laminar boundary layer as an inviscid, parallel shear flow subject to a steady, weak pressure disturbance. The equations were linearized and solved for a small perturbation of the pressure. In

reference 1, a portion of the supersonic boundary-layer flow was solved by the method of characteristics. This directly extended Lighthill's 1950 work to include strong disturbances while retaining the parallel shear-flow restriction. Fairly good agreement with surface pressure data and the location of incident and reflected shock waves was obtained for shock strengths below that which produced extensive separated regions, although viscous phenomena such as skin friction and heat transfer could not be predicted.

In 1953 Lighthill (ref. 3) extended his original model to account for the effects of viscosity near the wall in laminar boundary layers. This analysis was also based on a linearized theory for the outer, inviscid layer and the viscous effects were confined to an incompressible, inner layer. The method, as formulated in reference 3, did not consider separated flows. This shortcoming was overcome in Stewartson and Williams' (ref. 4) extension of Lighthill's two-layer model. Unfortunately, the analysis of reference 4 for laminar boundary layers was limited by assumption to very large Reynolds numbers (10^7 to 10^8). When the method is applied to interactions occurring at Reynolds numbers typical of those for which laminar boundary-layer data are available (less than 10^6), the predicted results do not agree with the data in the initial portion of the pressure rise. Reference 4 removed the restriction of a linearized solution in the outer layer present in the analysis of reference 3; however, predictions for the external flow field resulting from the interaction were not shown, and it was not stated how such a prediction could be obtained from that method.

In contrast to the two-layer models mentioned above, certain single-layer models (*e.g.*, refs. 5-8) treat the interaction as a completely viscous phenomenon using the boundary-layer equations and a Prandtl-Meyer equation to describe the inviscid flow outside the viscous layer. However, a critical evaluation (ref. 9) showed all four of these single-layer methods were unable to predict adequately interactions having large pressure rises.

For turbulent boundary-layer interactions, most methods are based on "control volume" models (*e.g.*, refs. 10 and 11) or on semiempirical techniques, such as that of reference 12, rather than on analytical solutions of the governing differential equations. These methods treat the interaction as a boundary-layer problem and yield little of the external flow-field information required for analyzing internal flows.

The purpose of this paper is to extend the analysis of reference 1 to account for the effects of viscosity for either a laminar or turbulent boundary layer. A two-layer model is employed which consists of an inner laminar boundary layer coupled to an outer rotational, inviscid layer. The method by which the viscous and inviscid flows are coupled is discussed in the text. The only empirical information required to complete the analysis of the interaction is a correlation for the extent of the upstream influence of the pressure rise. This correlation is discussed in the appendix.

The proposed method of analysis provides boundary-layer profiles, skin-friction, heat-transfer, and surface-pressure distributions throughout the interaction. The method also provides the strength and location of the reflected expansion and compression regions. Results obtained by this method are compared with experimental data for shock-wave interactions with both laminar and turbulent boundary layers.

DISCUSSION OF ANALYTICAL METHOD

Background

The method presented in reference 1 has been applied to interactions of oblique shock waves with turbulent boundary layers. Examination of the results indicated that further investigation of the two-layer model of the boundary layer in the interaction region was warranted.

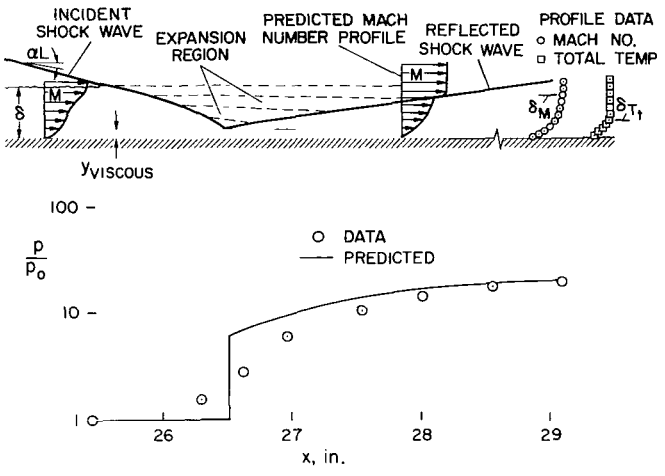

Figure 1.– Prediction of analytic method of reference 1; turbulent boundary layer, $M_o = 8.4$, $\alpha_L = 10°$ data from study of reference 13.

Two important results obtained from the method of reference 1 are illustrated in figure 1. The first is that a large expansion region is formed as the incident shock passes through the outer portion of the boundary layer. The expansion region has been observed in schlieren photographs of high Mach number, turbulent boundary-layer interactions (*e.g.*, figs. 5, 17, and 18 of ref. 13). This region is important since it affects the resulting external flow and the configuration of the reflected shock wave. Except for the method given in reference 1, current methods of analyzing shock-wave interactions with turbulent boundary layers do not account for the presence of an expansion region.

The second result is illustrated by comparing the predicted and experimental profiles downstream of the reflected shock wave shown in figure 1. The predicted Mach number profile is in general agreement with the experimental profile data obtained at a station slightly downstream of the predicted profile. The experimental total-temperature profile at the same station indicates that the viscous boundary-layer thickness (δ_{T_t}) is only about half of the thickness of the shear layer (δ_M). The predicted shear-layer thickness agrees with the experimental thickness, and it should be emphasized that this prediction was made solely from inviscid effects, neglecting any viscous mixing phenomenon.

Also in figure 1 the pressure distribution predicted by the method of reference 1 is compared with the experimental pressure distribution; the pressure data are shown to the same scale and properly alined with the flow-field sketch. The discrepancy in the predicted and experimental pressure distributions in the vicinity of the shock impingement point is the result of neglecting viscous effects.

It is thus apparent that the method of reference 1 can be used to predict many of the observable interaction features, but that it yields no information regarding viscous effects, such as skin friction and heat transfer. Furthermore, it yields no information as to the character of the

expansion and compression regions caused by the mutual interaction of the viscous and inviscid portions of the boundary-layer flow that have been observed in schlieren pictures.

The Coupled Two-Layer Model

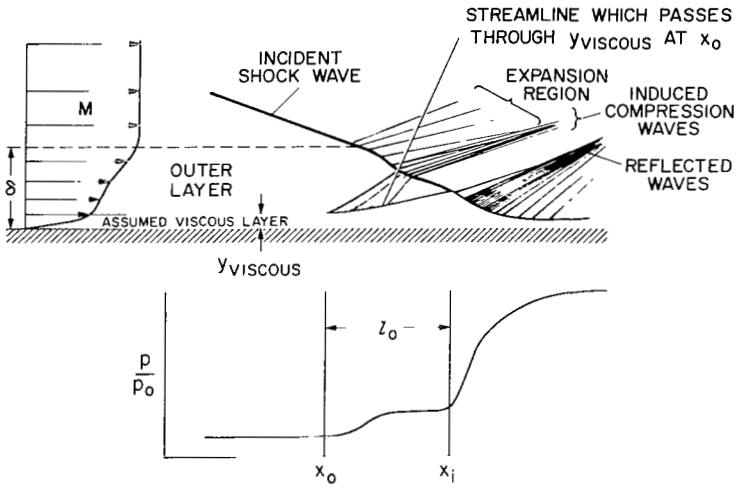

Figure 2.– Schematic diagram of two-layer model.

An extension of the method of reference 1 was undertaken to correct the shortcomings noted in the preceding section. The interaction model proposed in the present study is shown schematically in figure 2. Although the entering Mach number profile, shown at the upper left of the figure, is typical of that for a turbulent boundary layer, the present flow model is the same whether the boundary layer is turbulent or laminar. The model differs from that considered in reference 1 in some features, but retains the basic hypothesis that the boundary layer in the interaction region may be divided into two distinct regions. The outer layer is considered to be an inviscid, rotational, isoenergetic region in which normal (*i.e.*, transverse) pressure gradients may exist and in which any effects of viscosity and turbulent mixing are neglected. The inner layer is considered to be a laminar, viscous layer. It is also assumed that the entering Mach number profile may be used to determine the relative extent of the outer, or inviscid, layer, and the inner, or viscous, layer (*i.e.*, the height $y_{viscous}$ indicated in fig. 2). The method used is to determine the portion of the entering profile that will not significantly deform in the absence of viscous effects. This is done by integrating the inviscid equations downstream with a zero streamwise pressure gradient with the entering profile as initial data. The procedure can be illustrated by the use of figure 3. A typical turbulent boundary-layer profile entering an interaction region is shown by the solid line. The dashed curves represent three profiles, each obtained from an inviscid computation for a distance of five boundary-layer thicknesses downstream of the entering profile. This distance is used because it is typical of interaction lengths for turbulent flow. Each profile represents a different choice of $y_{viscous}$. It is clear that 0.03 inch is too low since the profile deforms excessively from the entering profile. This behavior is characteristic of a $y_{viscous}$ low

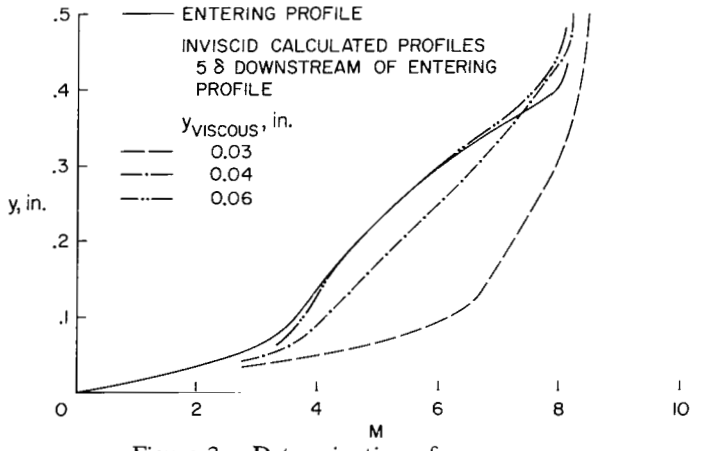

Figure 3.– Determination of $y_{viscous}$.

enough to encompass a portion of the profile that maintains its shape primarily through the effects of viscosity. A $y_{viscous}$ of 0.04 inch is slightly better than 0.03 inch but still is considered unacceptable for present purposes. On the other hand, $y_{viscous} = 0.06$ inch is considered acceptable because the profile has not changed significantly from the entering profile. As in reference 1, $y_{viscous}$ must still be chosen so that the flow downstream of the reflected shock remains supersonic. For the data examined in this study, the value of $y_{viscous}$, determined as outlined above, was sufficiently large that no subsonic flow downstream was encountered for turbulent boundary-layer flows with edge Mach numbers of 3.0 or greater. The occurrence of subsonic flow, of course, depends on the shock strength, but for shock strengths not excessively above that required for incipient separation, no problem is anticipated. The procedure described above for determining $y_{viscous}$ has the feature of providing a division between the inner and outer layers that is consistent with the approximation that viscous effects can be neglected in the outer layer. This procedure gives the minimum value for $y_{viscous}$ and is, therefore, the most desirable since it allows a maximum of the entering flow to be treated as inviscid.

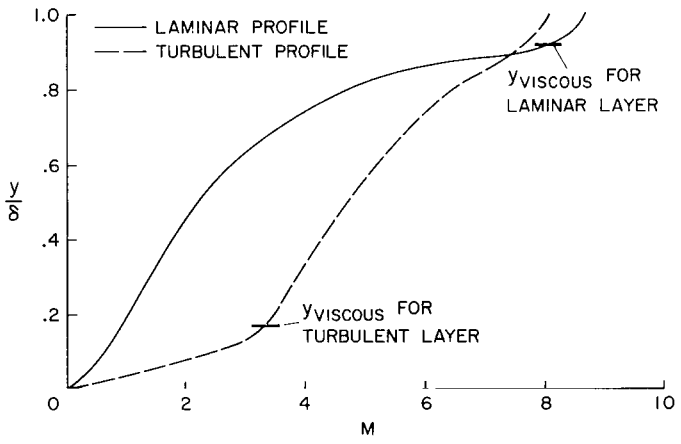

Figure 4.– Comparison of $y_{viscous}$ for laminar and turbulent boundary layers.

The above discussion was concerned with a turbulent entering boundary layer. An identical procedure may be applied for an entering laminar boundary-layer profile. Figure 4 shows the turbulent profile discussed in figure 3 with its $y_{viscous}$ and a typical laminar profile with its $y_{viscous}$ chosen just as above. The profiles are shown as y/δ versus Mach number to indicate the relative portion of the boundary layer (independent of its absolute thickness) that may be considered essentially inviscid. It can be seen that the percentage of the turbulent boundary-layer thickness in which viscous effects are neglected is much larger than that of the laminar layer.

The procedure outlined above is somewhat subjective and, therefore, the particular choice of $y_{viscous}$ might affect the solution of the interaction problem. Large changes in profile such as shown for $y_{viscous} = 0.03$ inch in figure 3 should definitely be avoided, while those associated with either $y_{viscous} = 0.04$ or 0.06 inch will not significantly affect the solution. For laminar flow, $y_{viscous}$ is nearly the boundary-layer thickness, and for all practical purposes may be taken as the boundary-layer thickness without significantly affecting the solution.

Subsequent to the determination of $y_{viscous}$, the combined inviscid and viscous entering profile to be used in the computation of the combined flows must be determined. For a laminar boundary layer this is quite simple. The viscous portion is just the portion of the entering boundary below $y_{viscous}$ and the outer inviscid layer is taken to be the remainder of the profile above $y_{viscous}$ plus a portion of the flow external to the boundary layer. The combined entering

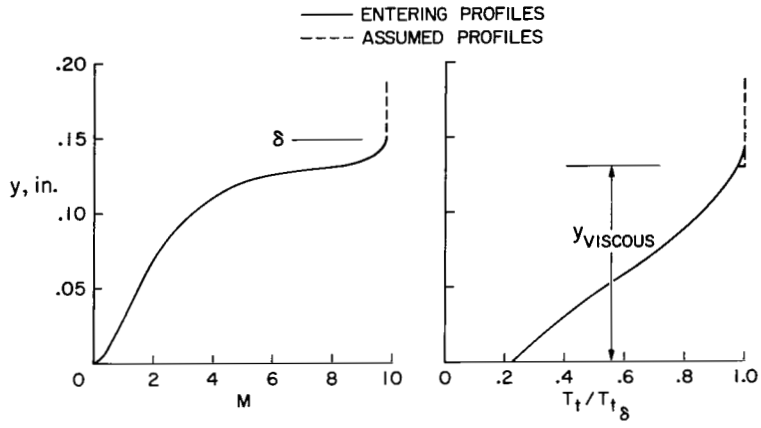

(a) Laminar boundary layer.

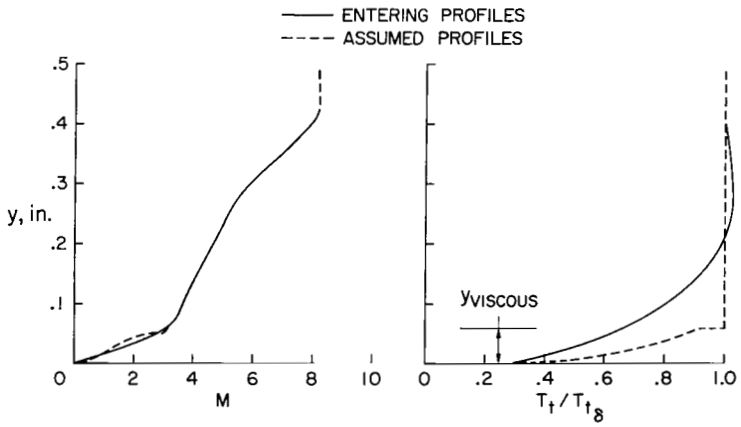

(b) Turbulent boundary layer.

Figure 5.– Composite entering profiles.

profile for a typical laminar boundary layer is shown in figure 5(a). Both the Mach number and total-temperature profiles shown can be obtained from any one of the methods of references 5, 6, 7, or 8. The Mach number profile is matched identically, while the assumed total-temperature profile has a slight discontinuity at $y_{viscous}$ because the outer layer is assumed isoenergetic.

The case of a turbulent entering profile is slightly different. For purposes of the present study, it is assumed that the viscous effects important in the interaction region can be represented by a laminar, inner layer. This assumption leads to the following technique for obtaining the assumed entering profile. The entering profiles, obtained in the experimental investigation of reference 13, are shown in figure 5(b) to illustrate the procedure. The portion of the turbulent entering profile is above $y_{viscous}$ and the Mach number profile is matched exactly for this portion. The viscous layer is assumed to be a laminar boundary layer with an edge Mach number equal to that of the local Mach number at $y_{viscous}$ and with the same wall shear as the entering turbulent profile. Zero pressure gradient is assumed in the axial direction. The scale of the inner layer is fixed by introducing a fictitious unit Reynolds number for the laminar boundary-layer edge so that the thickness of the inner layer is equal to $y_{viscous}$. The assumed Mach number profile below $y_{viscous}$ thus differs slightly from the experimental entering profile, and the gradients at $y_{viscous}$ are not matched. This procedure yields the assumed total-temperature profile shown in figure 5(b). The slight deviation of the assumed Mach number profile in the inner layer from the measured profile is probably within the experimental accuracy of determining profiles near the wall. The assumed and measured total-temperature profiles, however, are considerably different. The errors introduced by this discrepancy were not estimated in this study.

For further discussion, it is convenient to divide the interaction into upstream and downstream portions. The division is made at station x_i in figure 2, the point where the incident shock wave impinges on the outer edge of the viscous layer. The manner of selecting the outer edge of the viscous layer is discussed next; a more detailed description of determining x_i is given in the appendix.

It is assumed that upstream of x_i, the viscous layer, constituted as described above, may be treated as a free interaction problem and solved by any of the analytical computing programs described in references 5, 6, 7, and 8 once x_o is specified. The legnth l_o, which is the distance from the onset of the pressure rise x_o to the station x_i (fig. 2), can be obtained from experimental data by the procedure outlined in the appendix.

After the length of upstream influence is determined, a free-interaction solution for the viscous, inner layer is obtained from which the lower boundary of the outer layer is then taken. Many possible boundaries can be taken from the inner solution; these include the displacement thickness surface, the boundary-layer edge, or some appropriately chosen streamline. The latter was chosen for the present study since the method-of-characteristics computing program employed has a streamline as its lower boundary. Therefore, the mass flow will be conserved from the wall to any streamline in the outer flow. There is a slight inconsistency in choosing a streamline for the boundary since, in the inviscid outer flow, the total pressure is constant along a streamline ahead of the shock and discontinuously decreases to another constant level downstream of the shock, whereas in the viscous flow the total pressure decreases continuously along a streamline. The magnitude of this decrease, or its possible effects, were not assessed in the present study. The streamline chosen in the present study passes through a point that is the same distance from the wall as the height $y_{viscous}$ at station x_o. (See fig. 2.) The shape of this line determines the configuration of the induced compression wave and, hence, the predicted surface-pressure distribution. As pointed out in reference 9, two methods (refs. 5 and 6), one employing the displacement thickness line as the coupling line and the other employing the local boundary-layer edge, give essentially the same pressure distribution and hence must cause essentially the same turning of the inviscid flow. The streamline chosen in this study was located between the displacement thickness line and the boundary-layer edge for the viscous layer in all cases considered. Hence, the turning caused in the outer flow by this streamline is essentially the same as that in references 5 and 6. In summary, it should be noted that upstream of x_i, it is assumed that the viscous layer turns the outer flow and that the outer layer has no effect on the solution of the inner layer.

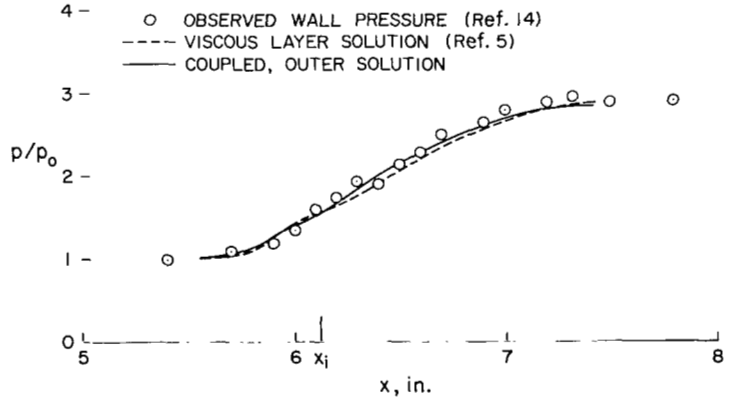

Figure 6.– Comparison of predicted and experimental surface-pressure distributions; $M_o = 9.7, \alpha_L = 2.2°$.

When one considers the flow downstream of x_i, the interaction between the inner and outer flows requires a slight modification of the procedure outlined for the flow upstream of x_i. This can be demonstrated by the following two results: The first is for the case of a relatively weak shock wave interacting with a laminar boundary layer, and the second is for a stronger shock interacting with the same boundary layer. Figure 6 shows the surface-pressure distribution data obtained from reference 14 for a weak interaction between a laminar boundary layer and a shock wave. The predicted surface-pressure distribution

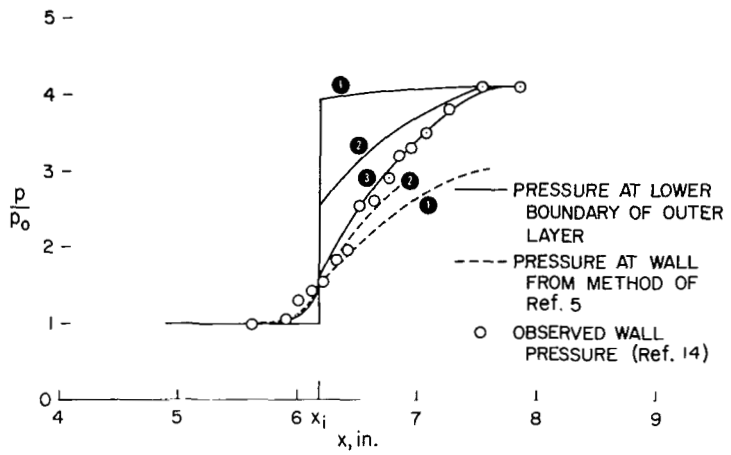

Figure 7.– Comparison of predicted and experimental surface-pressure distributions; $M_o = 9.7$, $\alpha_L = 3.2°$.

obtained from the method of reference 5 by matching x_o and x_i is indicated by the dashed curve. In this case the solution reaches the correct final pressure and satisfies the imposed downstream boundary conditions (*cf.* ref. 9). The streamline through $y_{viscous}$ at x_o was obtained from this solution and was used as the lower boundary of the outer flow. The outer flow was then solved for by the method of characteristics. The pressure distribution obtained from this solution is shown by the solid curve in figure 6. The agreement between the predicted pressures and the data both upstream and downstream of x_i is quite good, but not when the shock strength is increased, as shown in figure 7. The upstream-influence length is matched in the viscous solution (shown by the dashed curve labeled 1) and the resultant final pressure level underpredicts the data, a behavior discussed in detail in reference 9. In order to determine the reason for this failure and suggest a possible remedy the following procedure was followed. The streamline for the lower boundary of the inviscid solution was taken as before. The resulting surface-pressure distribution from the outer layer (shown by the solid curve labeled 2) agrees reasonably well with the data and the inner solution only to the shock impingement point. At shock impingement a discontinuity is evident in the outer layer pressure distribution. The solution to the inner layer corresponds to too weak an incident shock and the flow angle immediately downstream of the incident shock in the outer layer on the matching streamline was not the same as that given by the inner solution. This causes the reflection of a discrete shock wave and the resulting pressure discontinuity. An iterative procedure between the inner and outer solutions was required to obtain consistency in flow angle and thereby eliminate the pressure discontinuity. The broken curve labeled 2 in figure 7 is the result of imposing on the inner solution the flow angle at x_i taken from the solid curve labeled 2. The inner and, hence, the outer solutions upstream of x_i are not changed by this modification. The matching streamline is then taken from this inner solution as the lower boundary for the next outer solution. The procedure is convergent and may be continued until the pressures from the inner and outer solutions agree. A converged solution is shown by the curve labeled 3. One difficulty with this procedure is that the inner solution does not satisfy the imposed downstream boundary condition (ref. 5, 6, 7, or 8). Therefore, the inner solution stops short of both the final pressure level and the end of the interaction region, but continues at least to the reattachment point. It is numerically possible to surmount this difficulty by one of the following techniques. Downstream of reattachment, the pressure distribution for the inner layer may be prescribed as that obtained from the outer layer solution, and the solution can pass through the remaining downstream region without further difficulty. In the present study, the slope of the matching streamline was smoothly extrapolated from its value at the termination of the inner solution to a value of zero at the station where the final surface pressure is realized in the outer flow solution.

COMPARISON OF ANALYTICAL AND EXPERIMENTAL RESULTS

Some preliminary results obtained by the present method are compared in the following sections with experimental results obtained for interactions with laminar and turbulent boundary layers.

Flow-Field Characteristics

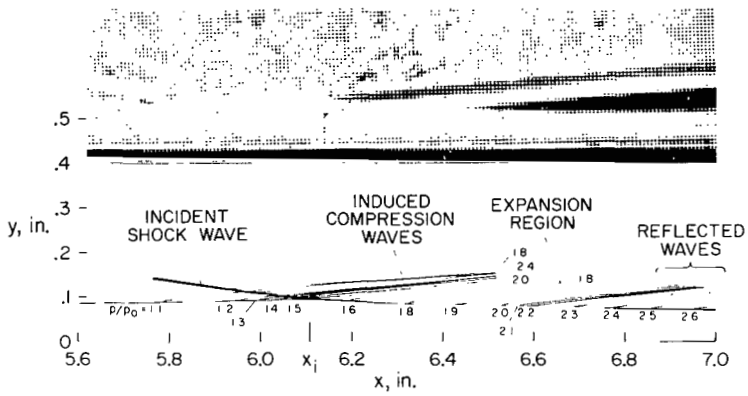

Figure 8.– Comparison of predicted and experimental shock-wave configuration for laminar flow (ref. 14); $M_o = 9.7, \alpha_L = 2.2°$.

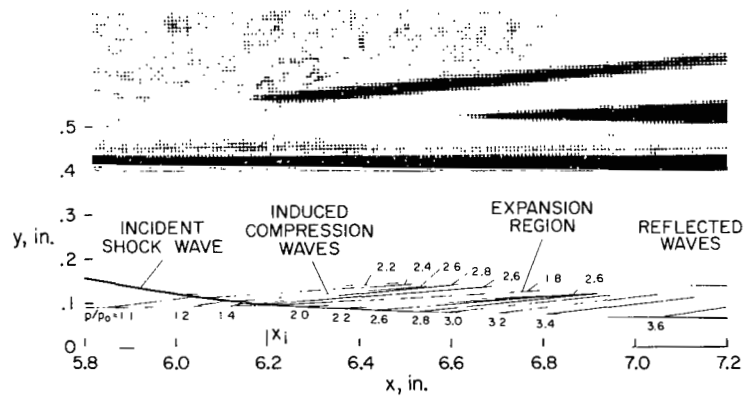

Figure 9.– Comparison of predicted and experimental shock-wave configuration for laminar flow (ref. 14); $M_o = 9.7, \alpha_L = 3.2°$.

Flow-field characteristics obtained by the present method for an interaction with a laminar boundary layer are presented in figure 8. Also shown for comparison is the schlieren photograph of the interaction taken from reference 12. The interaction considered here is the same as that for which the surface-pressure distribution was given in figure 6 ($M_o = 9.7$, $\alpha_L = 2.2°$). The predicted isobars (p/p_o = constant) from the coupled analysis are shown in the sketch of figure 8. The formation of the induced compression waves, expansion region, and reflected waves are in good qualitative agreement with the observable features of the schlieren photograph. The predictions of the surface-pressure distribution throughout the interaction region are also in good agreement, as shown in figure 6.

The flow-field predictions for the interaction corresponding to those conditions given in figure 7 ($M_o = 9.7$, $\alpha_L = 3.2°$) are compared with the schlieren photograph in figure 9. The analytical results also indicate good qualitative agreement with the observed features. The iterative procedure outlined in the discussion was needed to establish the downstream flow angle for the interaction presented in figure 9, whereas in figure 8, no iteration was required. Without the iterative procedure, the analytical results would have shown a discrete reflected shock rather than the broad compression region seen in both the schlieren photograph and converged analytic solutions.

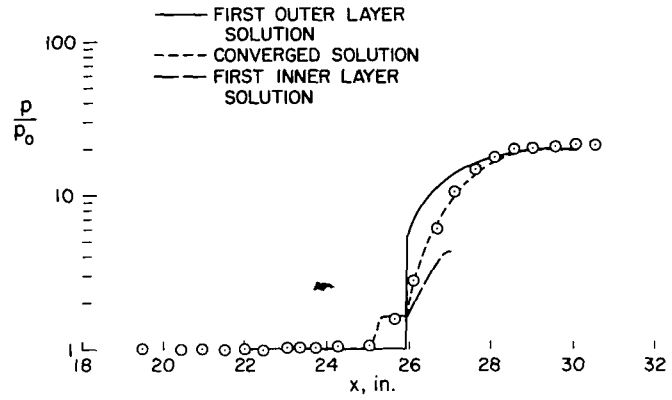

Figure 10.– Comparison of predicted and experimental pressure distribution for turbulent flow (ref. 13); $M_0 = 8.4, \alpha_L = 10°$.

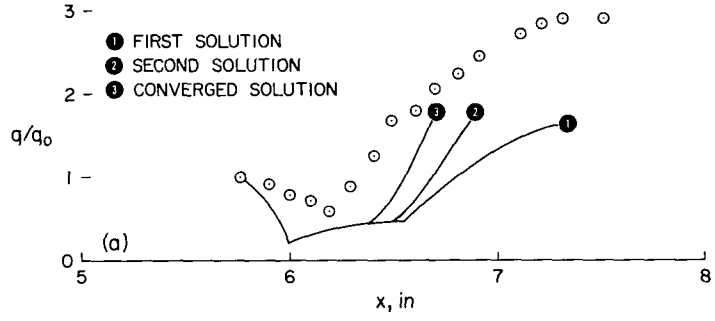

(a) Method of reference 5.

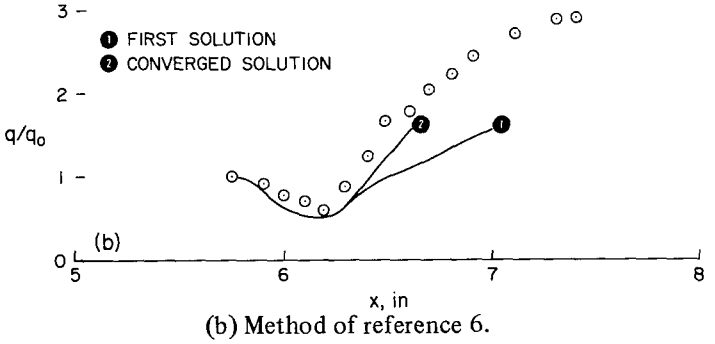

(b) Method of reference 6.

Figure 11.– Comparison of predicted and experimental heat-transfer rates for laminar flow; $M_0 = 9.7, \alpha_L = 3.2°$.

Comparisons between surface-pressure data for laminar flow and predicted pressures from the coupled method are shown in figures 6 and 7. For a turbulent flow case, the interaction data considered in figure 1 are compared in figure 10 with the prediction of the present method. The previously discussed iterative procedure was required to obtain the converged solution shown. A small separated region is predicted, but the spacing of the experimental data precluded any assessment of the validity of this prediction.

The results of heat-transfer predictions compared with the laminar boundary-layer data considered in figures 7 and 9 are presented in figure 11. The results obtained from the computing program of reference 5 are shown in figure 11(a). The curve labeled 1 is the solution without iteration on the downstream flow angle, while the curve labeled 2 is the result from the second iteration, and the curve labeled 3 is the result from the converged solution. The iterative procedure brings both the magnitude and gradient of the predicted heat-transfer rate into better agreement with experimental data. Similar results, shown in figure 11(b), were obtained by the method of reference 6. The heat-transfer predictions obtained with the method of reference 6 agree somewhat better with the data than those obtained with the method of reference 5. No comparisons have been made in the present study of heat-transfer rates in a turbulent-boundary – shock-wave interaction.

Skin-friction results are easily obtained from the present method; but since it is difficult to obtain C_f experimentally in interaction regions, no demonstrably reliable data are available for

comparison. However, a qualitative note concerning skin-friction behavior and the inferred separation length can be made on the basis of results obtained from the present method. The iteration procedure tends to shorten the distance from x_i to the point where the boundary layer reattaches, thus shortening the predicted length of the separated region. This shortening would bring the predictions of the viscous methods (refs. 5 and 6) into better agreement with experimentally observed separation lengths (see ref. 9), but no quantitative comparisons have been made at present.

CONCLUDING REMARKS

An effort was made to develop an improved analytical method for describing the details of the flow in the vicinity of a shock wave interacting with either a laminar or turbulent boundary layer. The method developed is useful in the study of the interaction of a shock wave and a boundary layer.

The analytical method employs the assumption that the boundary layer in an interaction can be divided into two distinct layers, one inviscid and the other viscous, and proposes a technique for coupling the two layers. This method adequately describes the characteristics of the flow field resulting from a shock-wave – boundary-layer interaction and predicts surface-pressure and heat-transfer distributions at least to the reattachment point.

Ames Research Center
National Aeronautics and Space Administration
Moffett Field, Calif., 94035, Aug. 12, 1970

APPENDIX A

THE EXTENT OF UPSTREAM INFLUENCE

GENERAL

The spreading of the pressure rise over several boundary-layer thicknesses upstream and downstream of the shock impingement location is a well-known feature of shock-wave – boundary-layer interactions. As noted in the text, information regarding the extent of upstream influence is required in order to use any of the existing analytical methods (refs. 5-8) to obtain a solution of the inner viscous layer as proposed in the present method. In order to make the comparisons between theory and data presented in the main text, a detailed examination of the specific data used was required. In particular, the extent of upstream influence taken from experimental data was used in the analysis. These data, together with data from several sources, were used to formulate correlations for the extent of upstream influence for both laminar and turbulent entering flows. These correlations, presented herein, may be used to obtain the length, l_o, when an analytical solution is desired but no experimental data are available.

Chapman, Kuehn, and Larson (ref. 15) used a weak-interaction analysis in studying the interaction of a shock wave and a boundary layer. When their analysis is used to determine the extent of upstream influence, a functional dependence of the form

$$\frac{l_o}{\delta_o} = f\left(C_{f_o} , \quad M_o , \quad \frac{p_p - p_o}{p_o}\right) \tag{A1}$$

is indicated. Attempts have been made to correlate existing data using equation (A1). Popinski and Ehrlich (ref. 16) considered wedge-induced interactions for both laminar and turbulent entering boundary-layer flows, and Popinski (ref. 17) considered externally generated shock waves interacting with turbulent boundary layers. Satisfactory correlations were not obtained in these studies since the deviation of some of the data from the recommended correlation curves is over 300 percent of the value given by the curves. Difficulty is encountered in employing the relation implied by equation (A1) because the plateau pressure p_p is, within experimental accuracy, constant for a given entering boundary layer. The extent of the upstream influence therefore cannot increase with increasing shock strength, a behavior that is inconsistent with experimental observation. To circumvent this difficulty in the present study, the functional form relating the important parameters of the problem is taken to be

$$\frac{l_o}{y} = f\left(C_{f_o} , \quad M_o , \quad \frac{p_{final} - p_o}{p_o}\right) \tag{A2}$$

where the reference length y is defined differently for laminar and turbulent flow.

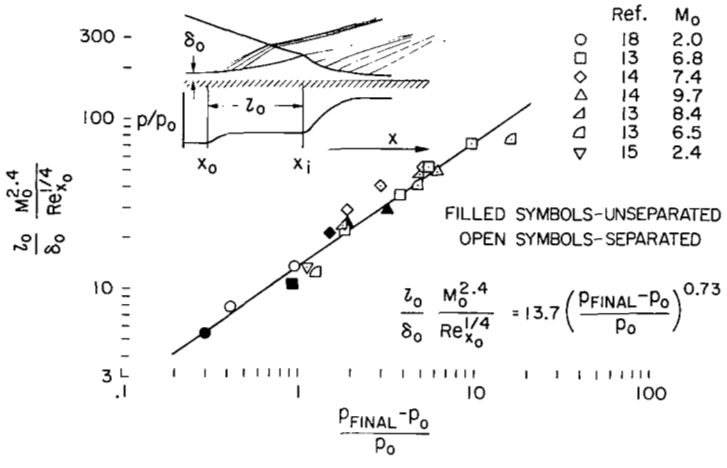

Figure 12. - Extent of shock-wave induced upstream influence for laminar boundary layers.

The correlation results for an interaction with an entering laminar boundary layer are presented in figure 12. The data shown were obtained from the interaction studies of references 13, 14, 15, and 18. The reference length, y, in equation (A2) is taken to be δ_0, the boundary-layer thickness at the onset of the pressure rise as indicated in the sketch of figure 12. The length, l_0, is the distance from the onset of the pressure rise to the station where the incident shock wave impinges on the edge of the boundary layer. The choice of this impingement point can be made with reasonable certainty with the aid of a schlieren photograph of the interaction. In connection with determining the impingement point, x_i, it is interesting to note that, within the experimental accuracy of the data examined, the end of the pressure plateau and the impingement point occurred at the same station. Note that, in general, this impingement point cannot be determined analytically from inviscid considerations alone, since the physical configuration of the incident shock wave is modified by the induced compression region ahead of shock impingement. However, using the coupled technique presented in the body of this report, one can analytically obtain the point x_i and, then, through the suggested correlation, obtain the length l_0 (and, hence, x_0). This is done by an iterative process: First, the outer layer is solved without any sublayer considerations, as was done in reference 1. This process yields a first approximation to x_i. Next, a value for l_0 is obtained from the correlation by assuming that the value of Re_{x_0} is that of Re_{x_i}. The sublayer is then computed from one of the viscous interaction programs suggested in the main text. The resulting streamline through $y_{viscous}$ is employed as the lower boundary for the outer layer solution, as outlined in the main text. A different x_i results and the entire process is repeated until little or no change in the value of x_i is obtained from two successive calculations.

The functional form of the term involving C_{f_0} in equation (A2) is taken as $\sqrt{C_{f_0}}$ in agreement with the weak interaction analysis. For convenience the term $Re_{x_0}^{-1/4}$ has been substituted for $\sqrt{C_{f_0}}$ for the laminar case; M_0 is the boundary-layer-edge Mach number at the onset of the pressure rise.

It can be seen from figure 12 that these parameters adequately correlate the data for both separated and unseparated interactions over a wide range of Mach numbers and shock strengths for a range of Re_{x_0} from about 10^5 to 10^6. The largest deviation of the data from the recommended correlation equation

$$\frac{\ell_o M_o^{2.4}}{\delta_o Re_{x_o}^{1/4}} = 13.7\left(\frac{p_{final} - p_o}{p_o}\right)^{0.73} \tag{A3}$$

is about 30 percent, while most of the data are within 10 percent of the value given by the curve. Using the actual value of $\sqrt{C_{f_o}}$ instead of $Re_{x_o}^{-1/4}$ might reduce these deviations.

TURBULENT BOUNDARY LAYER

The thesis of the present work has been used to develop a set of parameters that give an adequate correlation for the extent of shock-induced upstream influence for turbulent layers. The reasoning that was used to select the parameters that might best describe the physical mechanism involved in the upstream propagation of the pressure rise is as follows. The forward propagation of the downstream disturbance must have its primary path in the subsonic flow adjacent to the wall. The effects of viscosity limit the extent of the upstream influence. The correct reference length in equation (A2), therefore, should be some height that encompasses the subsonic flow and above which the effects of viscosity may be neglected. Thus, in the present study, the height, $y_{viscous}$, obtained by the procedure outlined in the main text is taken as the reference length, since below $y_{viscous}$ the flow is primarily viscous and contains the subsonic region. For turbulent flow, x_i is taken as the station where the incident shock impinges on the local edge of the viscous sublayer, a procedure that is consistent with the laminar case. Experimental determination of this station is somewhat subjective, since no physical dividing line exists in the actual flow; however, schlieren photographs of the interaction can be employed to obtain the station x_i. For the purposes of the present study, the impingement point was taken from schlieren photographs at the position where the incident shock disappears within the lower portion of the boundary layer. This station is indicated in the sketch of figure 13.

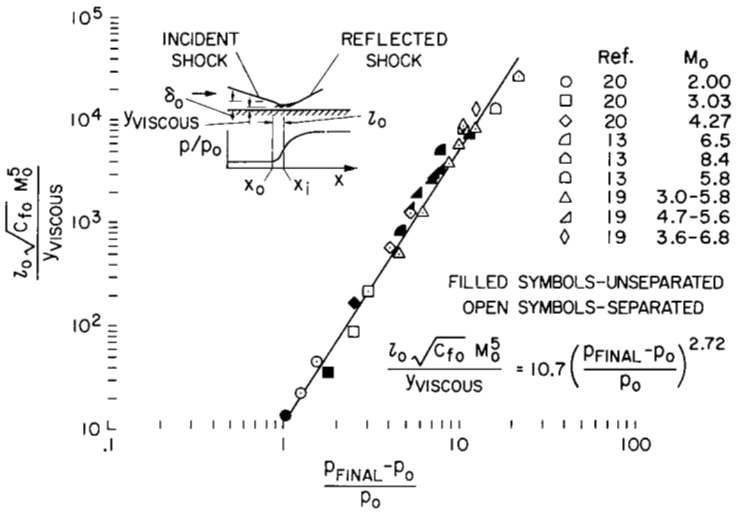

Figure 13.– Extent of shock-wave induced upstream influence for turbulent boundary layers.

The shock impingement station can be determined analytically by the iterative technique outlined for the laminar boundary layer in the previous section of this appendix. Note that in contrast to the laminar case, the term $\sqrt{C_{f_o}}$ is not replaced by its corresponding Reynolds number for the reasons outlined in reference 19. The values of C_{f_o} are obtained by employing a reference temperature method with the law-of-the-wall exactly as done in reference 19.

The data (from refs. 13, 19, and 20) are well correlated by the relation

$$\frac{l_o \sqrt{C_{f_o}}\, M_o^{5.0}}{y_{viscous}} = 10.7 \left(\frac{p_{final} - p_o}{p_o} \right)^{2.72} \tag{A4}$$

The maximum deviation of a data point from the recommended curve is about 50 percent while most of the data are within 20 percent of the curve. Equation (A4) represents a substantial improvement over previously existing correlation relationships.

REFERENCES

1. Rose, W. C.; Murphy, J. D.; and Watson, E. C.: Interaction of an Oblique Shock Wave With a Turbulent Boundary Layer. AIAA J., vol. 6, no. 9, Sept. 1968, pp. 1792-1793.

2. Lighthill, M. J.: Reflection at a Laminar Boundary Layer of a Weak Steady Disturbance to a Supersonic Stream Neglecting Viscosity and Heat Conduction. Quart. J. Mech. Appl. Math., vol. III, pt. 3, 1950, pp. 303-325.

3. Lighthill, M. J.: On Boundary Layers and Upstream Influence. II. Supersonic Flows Without Separation. Proc. Roy. Soc. A. 217, 1953.

4. Stewartson, K.; and Williams, P. G.: Self-Induced Separation. Proc. Roy. Soc. A. 312, 1969.

5. Goodwin, F. K.; Nielsen, J. N.; and Lynes, L. L.: Calculation of Laminar Boundary Layer-Shock Wave Interaction by the Method of Integral Relations. NEAR Rep. TR 2, Nielsen Engineering and Research, Inc., July 25, 1967.

6. Reyhner, T. A.; and Flügge-Lotz, I.: The Interaction of a Shock Wave With a Laminar Boundary Layer. Tech. Rep. 163, Div. Eng. Mech., Stanford Univ., Nov. 1966, published in abbreviated form in Int. J. Non-Linear Mech., vol. 3, no. 2, June 1968, pp. 173-199.

7. Lees, L.; and Reeves, B. L.: Supersonic Separated and Reattaching Laminar Flows: I. General Theory and Application to Adiabatic Boundary-Layer/Shock-Wave Interactions. AIAA J., vol. 2, no. 11, Nov. 1964, pp. 1907-1920.

8. Klineberg, J. M.: Theory of Laminar Viscous-Inviscid Interactions in Supersonic Flow. Ph. D. Thesis, Calif. Inst. Tech., June 1968.

9. Murphy, John D.: A Critical Evaluation of Analytic Methods for Predicting Laminar-Boundary-Layer Shock-Wave Interaction. Paper presented at the NASA Symposium on Analytic Methods in Aircraft Aerodynamics, Oct. 28-30, 1969.

10. Reshotko, Eli; and Tucker, Maurice: Effect of a Discontinuity on Turbulent Boundary-Layer-Thickness Parameters With Applications to Shock-Induced Separation. NACA TN–3454, 1955.

11. Seebaugh, William R.; Paynter, Gerald C.; and Childs, Morris E.: Shock-Wave Reflection From a Turbulent Boundary Layer With Mass Bleed. J. Aircraft, vol. 5, Sept.-Oct. 1968, pp. 461-467.

12. Pinckney, S. Z.: Semiempirical Method for Predicting Effects of Incident-Reflecting Shocks on the Turbulent Boundary Layer. NASA TN D–3029, 1965.

13. Watson, Earl C.; Murphy, John D.; and Rose, William C.: Shock-Wave Boundary-Layer Interactions in Hypersonic Inlets. Conference on Hypersonic Aircraft Technology, NASA SP–148, 1967, Paper 22.

14. Needham, D. A.: Laminar Separation in Hypersonic Flow. Ph. D. Thesis, Univ. of London, 1965.

15. Chapman, Dean R.; Kuehn, Donald M.; and Larson, Howard K.: Investigation of Separated Flows in Supersonic and Subsonic Streams With Emphasis on the Effect of Transition. NACA Rep. 1356, 1958.

16. Popinski, Z.; and Ehrlich, C. F.: Development Design Methods for Predicting Hypersonic Aerodynamic Control Characteristics. AFFDL TR-66-85, Lockheed California Co., Sept. 1966.

17. Popinski, Z.: Shock-Wave Boundary-Layer Interaction. Rep. LR 18307, Lockheed California Co., 29 June 1965.

18. Hakkinen, R. J.; Greber, I.; Trilling, L.; and Abarbanel, S. S.: The Interaction of an Oblique Shock Wave With a Laminar Boundary Layer. NASA Memo 2-18-59W, 1959.

19. Watson, E. C.; Rose, W. C.; Morris, S. J.; and Gallo, W. F.: Studies of the Interaction of a Turbulent Boundary Layer and a Shock Wave at Mach Numbers Between About 2 and 10. Compressible Turbulent Boundary Layers, NASA SP–216, 1969, Paper 20.

20. Pinckney, S. Z.: Data on Effects of Incident-Reflecting Shocks on the Turbulent Boundary Layer. NASA TM X–1221, 1966.

NASA-Langley, 1970 —— 12 A-3714

"The aeronautical and space activities of the United States shall be conducted so as to contribute . . . to the expansion of human knowledge of phenomena in the atmosphere and space. The Administration shall provide for the widest practicable and appropriate dissemination of information concerning its activities and the results thereof."

— NATIONAL AERONAUTICS AND SPACE ACT OF 1958

NASA SCIENTIFIC AND TECHNICAL PUBLICATIONS

TECHNICAL REPORTS: Scientific and technical information considered important, complete, and a lasting contribution to existing knowledge.

TECHNICAL NOTES: Information less broad in scope but nevertheless of importance as a contribution to existing knowledge.

TECHNICAL MEMORANDUMS: Information receiving limited distribution because of preliminary data, security classification, or other reasons.

CONTRACTOR REPORTS: Scientific and technical information generated under a NASA contract or grant and considered an important contribution to existing knowledge.

TECHNICAL TRANSLATIONS: Information published in a foreign language considered to merit NASA distribution in English.

SPECIAL PUBLICATIONS: Information derived from or of value to NASA activities. Publications include conference proceedings, monographs, data compilations, handbooks, sourcebooks, and special bibliographies.

TECHNOLOGY UTILIZATION PUBLICATIONS: Information on technology used by NASA that may be of particular interest in commercial and other non-aerospace applications. Publications include Tech Briefs, Technology Utilization Reports and Notes, and Technology Surveys.

Details on the availability of these publications may be obtained from:

SCIENTIFIC AND TECHNICAL INFORMATION DIVISION

NATIONAL AERONAUTICS AND SPACE ADMINISTRATION

Washington, D.C. 20546